Chinese Chemical Letters 35 (2024) 109262

Contents lists available at ScienceDirect

Chinese Chemical Letters

journal homepage: www.elsevier.com/locate/cclet

# Enhanced degradation of refractory organics in ORR-EO system with a blue $TiO_2$ nanotube array modified Ti-based Ni-Sb co-doped $SnO_2$ anode

Yifen He[a], Chao Qu[a,b,*], Na Ren[a], Dawei Liang[a]

[a] Department of Materials Chemistry, School of Materials Science & Engineering, Beihang University, Beijing 102206, China
[b] Department of Environmental Science, Faculty of Environment & Life, Beijing University of Technology, Beijing 100124, China

ARTICLE INFO

*Article history:*
Received 3 August 2023
Revised 6 October 2023
Accepted 26 October 2023
Available online 30 October 2023

*Keyword:*
Electro-oxidation
Blue $TiO_2$ nanotube array
$O_3/H_2O_2$ process
Refractory organics
Leachate bio-effluent

ABSTRACT

Recently, a novel 2-electron oxygen reduction reaction (ORR) based electro-oxidation (EO) system was developed, which utilizes a $H_2O_2$ generation cathode instead of $H_2$ evolution cathode. A Ti-based Ni-Sb co-doped $SnO_2$ (Ti/NATO) anode was selected for efficient degradation of refractory organics and $O_3$ production. The synergistic reaction of $O_3/H_2O_2$ further accelerated the generation of hydroxyl radicals ($^{\bullet}OH$) in the ORR-EO system. However, the catalytic activity and long-term effectiveness of the Ti/NATO anode limited the large-scale application of the ORR-EO process. In this study, a blue $TiO_2$ nanotube array (blue-$TiO_2$-NTA) inter-layer was introduced into the fabrication process between the Ti substrate and NATO catalyst layer. Compared to the Ti/NATO anode, the Ti/blue-$TiO_2$-NTA/NATO anode achieved higher efficiency of organic removal and $O_3$ generation. Additionally, the accelerated lifetime of the Ti/blue-$TiO_2$-NTA/NATO anode was increased by 7 times compared to the Ti/NATO anode. When combined with CNTs-C/PTFE air cathode in ORR-EO system, all anodic oxidation and $O_3/H_2O_2$ processes achieved higher $^{\bullet}OH$ production. Over 92% of TOC in leachate bio-effluent was effectively eliminated with a relatively low energy cost of 45 kWh/t.

The increasing discharge of industrial refractory organic wastewater, such as dye [1], pharmacy [2], emerging contaminants [3] and landfill leachate [4], has drawn more and more attention of the government and society due to its serious environmental risks. Since the traditional biochemical methods are limited by the high organic concentration, toxicity, and salinity [5], advanced oxidation processes (AOPs) have been developed rapidly in recent years, due to its ability to generate hydroxyl radicals ($^{\bullet}OH$) with high oxidation potential (2.80 eV) for the degradation of organic matters [6].

Among all kinds of AOPs, electro-oxidation (EO) process with the advantages of high energy efficiency, fast reaction speed, strong environmental adaptability, simple structure, stable operation conditions, no-additional chemicals required, was considered as one of the most promising AOPs in the future [7]. The most difficult problem of EO process was the high materials cost and energy cost, so it became a hot topic for researchers to develop novel energy-saving EO process and efficient and stable electrode materials [8].

Previously, a carbon nanotubes coated carbon black and polytetrafluoroethylene (CNTs-C/PTFE) air cathode combined with a titanium based nickel and antimony doped tin oxide (Ti/NATO) anode was proved to be efficient and energy-saving for removing refractory organics in an EO system [9,10]. As shown in Fig. 1, CNTs-C/PTFE air cathode was effective for $H_2O_2$ generation through a 2-electron oxygen reduction reaction (ORR) and Ti/NATO anode owned excellent anodic oxidation and $O_3$ generation ability, so called ORR-EO. ORR-EO not only decreased the applied voltage by changing cathodic hydrogen evolution reaction (HER) into ORR, but also accelerated $^{\bullet}OH$ generation through synergistic $O_3/H_2O_2$ process [11,12].

However, due to the limited amount of $O_3$ produced by the Ti/NATO anode, which is much lower than the amount of $H_2O_2$ produced by the cathode, there is no strong peroxone effect in the ORR-EO system. In addition, the main limitation against the large-scale industrial application of Ti/NATO anode is the low service life [13]. Therefore, there is an urgent need to improve the efficiency of $O_3$ production and lifetime of Ti/NATO anode [14]. With the rapid developing and wide research on Ti based dimensional stable anode (DSA) in recent years, one of the most useful methods to improve the lifetime of anode was modifying a highly ordered

---

* Corresponding author.
*E-mail address:* quchao@bjut.edu.cn (C. Qu).

https://doi.org/10.1016/j.cclet.2023.109262
1001-8417/

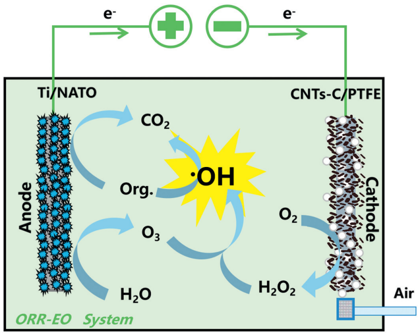

**Fig. 1.** Schematic diagram of ORR-EO system.

$TiO_2$ nanotube array ($TiO_2$-NTA) on Ti substrate by electrochemical anodizing method [15]. On one hand, by building micro 3D structure under the finite geometric area, $TiO_2$-NTA could increase the loading of catalysts, further improved the electrochemical activity of electrode [16]. On the other hand, $TiO_2$-NTA could increase oxygen evolution potential (OEP), which suppress the side reactions in the electrolysis process, and it can perfectly protect the Ti substrate and enlarge the lifetime of the electrode [17].

However, due to the weak electron conductivity of $TiO_2$, which is a wide bandgap semiconductor, the huge interface resistance will reduce the electron transfer from the catalyst layer to the Ti substrate [18]. More and more studies were working on reducing the ohm resistance of Ti/$TiO_2$-NTA while remaining the high efficiency for water treatment [19]. Such as achieving a Magnèli phase $Ti_4O_7$ from $TiO_2$ by $H_2$ reduction over 1000 °C [20] and fabricating a blue-$TiO_2$-NTA [21]. The conductivity of blue-$TiO_2$-NTA is proved to be enhanced by the doping of $Ti^{3+}$, which makes $TiO_2$-NTA present a blue color after electrochemical cathodic reduction under room temperature. So it is an efficient and inexpensive electrode material for EO wastewater treatment [22].

In this work, a blue-$TiO_2$-NTA inter-layer was introduced into the fabrication process for comprehensively improving the performance of Ti/NATO anode, including organics removal, $O_3$ generation, and lifetime. Combined with CNTs-C/PTFE air cathode, the organics removal efficiency of ORR-EO system was further improved. The morphology and element compositions were characterized by SEM, XRD and EDS, electrochemical properties of LSV was tested by electrochemical workstation. Accelerated lifetime test was performed to evaluate the stability of the electrode. Reactive oxygen species (ROS) including $O_3$, $H_2O_2$ and $^{\bullet}OH$ were detected to evaluate the reaction mechanisms in ORR-EO system. Finally, the wastewater treatment performances including TOC removal and energy cost were evaluated by treating phenol wastewater and landfill leachate bio-effluent in the Ti/blue-$TiO_2$-NTA/NATO anode and CNTs-C/PTFE cathode combined ORR-EO system.

The fabrication of Ti/blue-$TiO_2$-NTA/NATO anode includes the Ti mesh inner substrate layer, the blue-$TiO_2$-NTA intermediate supporting layer, and the NATO outer catalyst layer. Titanium (Ti) plate (99.5% pure, Changli Co., Ltd., Baoji, China) were applied as base metal with the dimension of 5 × 10 cm and thickness of 1 mm. First, the Ti mesh was polished by sandpaper with 200, 400, 800 and 2000 meshes in turn to remove the passivation layer, and then the Ti mesh was etched by boiling in 10% oxalic acid solution for 2 h to increase the surface area. Then the etched Ti mesh was washed with ultra-pure water and dried at room temperature.

A voltage of 20 V were applied on Ti mesh anode with a platinum sheet cathode (1 cm × 1 cm) in 0.5% HF solution for 20 min, and then the Ti mesh was annealed in a muffle oven at 450 °C for 3 h to obtain the Ti/$TiO_2$-NTA electrode. The prepared Ti/$TiO_2$-NTA electrode was used as cathode with a graphite anode in 1 mol/L $Na_2SO_4$ solution for 5 min (25 °C, cathodic current density 10 mA/cm$^2$) in a double electrode system to obtain a Ti/blue-$TiO_2$-NTA electrode. Finally, the NATO outer layer were prepared by the dip-coating and annealing method according to our previous report [23]. The coating solution contained $SnCl_4 \cdot 5H_2O$ (0.05 mol/L), $SbCl_3$, and $NiCl_2$ (Aladdin Reagent, Shanghai, China) with a mole ratio of Sn:Sb:Ni at 250:8:1 in 50 mL of ethanol, together with 2 mL HCl (37%, Aladdin Reagent, Shanghai, China) to prevent the hydrolysis of the solvent.

The oxygen evolution potential (OEP) of Ti/blue-$TiO_2$-NTA/NATO anode was tested by an electrochemistry workstation (CHI 660E, Chenhua Instruments, Shanghai, China) under linear sweep voltammetry (LSV) mode with a scan rate of 50 mV/s and a potential range of 0–3 V. The surface property and chemical composition of Ti/blue-$TiO_2$-NTA/NATO anode were conducted with a scanning electron microscope (SEM) (Sigma 500, ZEISS, Germany) and a diffraction of X-rays diffraction (XRD) (D8 Advance, Bruker, Germany) were obtained at a rate of 0.1 steps per second from 10° to 90°. The accelerated life test is carried out in 1 mol/L $H_2SO_4$ solution with constant current density of 1 A/cm$^2$, using Ti/blue-$TiO_2$-NTA/NATO electrode as anode and platinum sheet as cathode.

As described in a former work [3], the C/PTFE gas diffusion layer was prepared by mixing 1.6 g of carbon black powder (Baochi Chemical, Tianjin, China) with 4 g of 60% PTFE emulsion (DuPont, USA) and 5 mL of ethanol to make a carbon paste, which was then blended thoroughly and rolled into a thin film (30 µm in thickness) by a calendar press. The CNTs catalyst, with loading at 1 mg/cm$^2$, was brushed on the surface of C/PTFE film, with one side containing catalyst as the reaction surface, and the other side as the gas diffusion channel. Then the carbon film was sintered in a muffle oven at 340 °C for 30 min. The CNTs-C/PTFE cathode was prepared by enclosing two pieces of CNTs-C/PTFE electrode to a graphite frame (5 × 7 cm$^2$), with the catalyst side facing outwards. On both sides of the frame left a hole (Ø = 1.5 mm) for air flowing in and out of the air cathode to provide oxygen.

Phenol solution was prepared by dosing 200 mg of phenol and 14.2 g of $Na_2SO_4$ in 1 L deionized water. Each batch of electrolysis experiment was carried out by charging with 10 mA/cm$^2$ current density in 200 mL of phenol solution in a 250 mL glass beaker. Ti/NATO, Ti/$TiO_2$-NTA/NATO and Ti/blue-$TiO_2$-NTA/NATO anodes combined with the CNTs-C/PTFE air cathode (air flow rate = 200 mL/min) were used in a single electrolysis cell at a 1 cm distance. DC power was provided with battery testing equipment (10 V–10 A, Neware, Shenzhen, China). A 2 mL of sample was taken every 30 min for further HPLC (LC-20A, Shimazu, Japan) and TOC (Multi-C/N 2100, Jena, Germany) analysis.

The reactive oxygen species (ROS) including $O_3$, $H_2O_2$ and $^{\bullet}OH$ were conducted in a dual-chamber electrolysis cell. As illustrated in Fig. 2, Ti/blue-$TiO_2$-NTA/NATO anode and CNTs-C/PTFE cathode were separated with a cation exchange membrane (Nafion 211, Dupont, USA). $Na_2SO_4$ solution (150 mL, 0.1 mol/L) without organics was added to each chamber, and a current density of 10 mA/cm$^2$ was applied for electrolysis. $O_3$ generated in the anode chamber was measured through an iodometric method. The concentration of $H_2O_2$ in the cathode chamber was measured with potassium titanium oxalate spectrophotometry. The $^{\bullet}OH$ was analyzed by an ESR spectrometer (ESP-300E, Bruker, Germany). The spin-trapping agent of 5,5-dimethyl-1-pyrroline-*N*-oxide (DMPO) (Sigma-Aldrich Inc., USA) was applied for $^{\bullet}OH$ analysis. A 200 mmol/L DMPO solution was prepared by dissolving the chemicals into ultra-pure water for $^{\bullet}OH$ trapping. A 20 µL of DMPO was mixed with 180 µL of an anodic or cathodic solution, and then the mixed solution was sealed in a glass capillary for ESR analysis.

The bio-effluent used in this study was obtained from a landfill site in Beijing that has been operational for over 30 years. Prior to analysis, the landfill leachate was subjected to anaerobic and

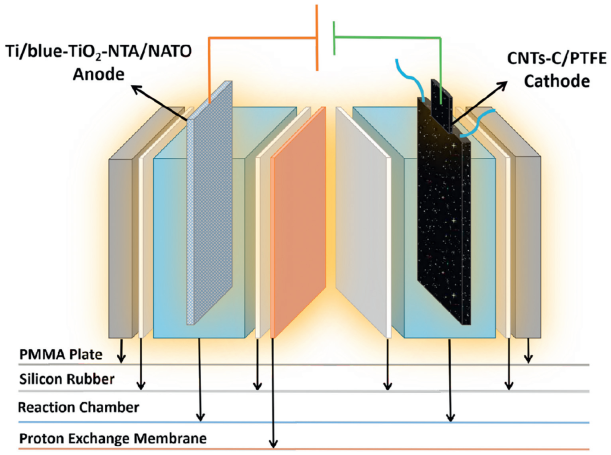

**Fig. 2.** Schematic diagram of the dual-chamber ORR-EO reactor.

**Table 1**
Characteristics of leachate bio-effluent.

| Parameters | Average value | Parameters | Average value |
|---|---|---|---|
| pH | 7.43 | TN (mg/L) | 1550 |
| Color | Dark brown | $Cl^-$ (mg/L) | 3670 |
| COD (mg/L) | 707.6 | $Ca^{2+}$ (mg/L) | 160 |
| TOC (mg/L) | 196.2 | $Mg^{2+}$ (mg/L) | 450 |
| TDS (mg/L) | 11,500 | EC (mS/cm) | 25.3 |

aerobic/anoxic treatment to remove biodegradable organics and nitrogen. The characteristics of the landfill bio-effluent are listed in Table 1. The bio-effluent was a dark brown liquid containing organics that were nearly non-biodegradable. Due to the high electrical conductivity of the concentrates (25.3 mS/cm), no additional supporting electrolyte was used during electrochemical treatment.

The ORR-EO system with Ti/blue-$TiO_2$-NTA/NATO anode and CNTs-C/PTFE cathode was operated under 10 $mA/cm^2$ of current density and air flow rate of 200 mL/min in a 250 mL glass beaker, for the treatment of a landfill leachate bio-effluent, which was obtained from a membrane bioreactor from a local landfill site. 200 mL of landfill leachate bio-effluent was treated in each batch and 2 mL sample was taken every 2 h for TOC analysis. The energy consumption was calculated following Eq. 1, where the Ec is energy consumption ($kWh/m^3$), $U$ is average cell voltage (3.6 V), $I$ is total current (0.25 A, 10 $mA/cm^2$ × 25 $cm^2$), $t$ is time (h) for 97% TOC removal and $V$ is the volume of solution (0.2 L).

$$Ec = U \cdot I \cdot t / V \tag{1}$$

The XRD profiles (Fig. 3) show the crystal structure of each layer including Ti substrate (Fig. 3a), $TiO_2$-NTA (Fig. 3b) and blue-$TiO_2$-NTA inter layer (Fig. 3c). Diffraction peaks located at 38.7°, 40.5°, 53.3°, 70.9°, 76.5°, and 77.7° can be used as indicators of the Ti base (JCPDS No. 65-3362). The main diffraction peak of $TiO_2$ is located at 25.4°, 37.0°, 37.9°, 38.7°, and 48.2° (ICDD 01-083-2243). Combined with Fig. 4a, it was proved to be $TiO_2$ NTA. However, the diffraction peak intensity and the crystallization was low, which makes hydrogen reduction can be made easier on such underdeveloped crystals. As shown in Fig. 3c, after the reduction, the anskase-type $TiO_2$ structure on the surface of interlayer is replaced by a titanium-hydrogenated blue-$TiO_2$ structure (ICDD 01-078-22160, and the diffraction peak is located at 35.3°, 40.9°, 59.4°, 70.9°, and 74.6°).

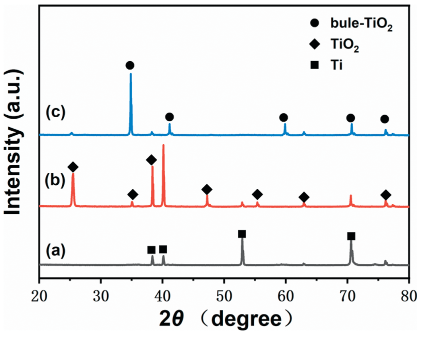

**Fig. 3.** XRD profiles of the (a) Ti substrate, (b) $TiO_2$-NTA, and (c) blue-$TiO_2$-NTA inter layer.

The SEM images show the blue-$TiO_2$-NTA (Fig. 4a) was highly ordered on the Ti mesh substrate which the averaged diameter is about 100 nm. And nano-scaled NATO catalyst particles were evenly loaded on the blue-$TiO_2$-NTA inter layer (Fig. 4b). As shown in Fig. 4c, the EDS image shows the Sn, Sb, Ni, and O elements in NATO catalyst layer were evenly distributed on the surface of blue-$TiO_2$-NTA inter layer.

The prepared Ti/NATO, Ti/$TiO_2$-NTA/NATO and Ti/blue-$TiO_2$-NTA/NATO anodes were analyzed as the working electrode, with a Pt plate (1 $cm^2$) as the counter electrode and a saturated calomel electrode (SCE, 0.241 V *vs.* NHE) as the reference electrode. The LSV tests of the electrodes were executed in a 0.1 mol/L $Na_2SO_4$ solution at pH 7.

As shown in Fig. 5a, the LSV profiles demonstrated that all the anodes own a high oxygen evolution potential (OEP) at around 2.0 V *vs.* SHE. The high OEP indicate all the anodes could degrade organics with less side-reactions. The LSV curve of Ti/NATO anode shows a higher current density compared to that of Ti/$TiO_2$-NTA/NATO anode, due to the resistance introduced by $TiO_2$-NTA as a semi-conductor. It will cause the increase of the applied voltage at a certain current density while treating wastewater. After modified by electrochemical cathodic reduction, the Ti/blue-$TiO_2$-NTA/NATO anode recovered the current density and even better than Ti/NATO anode. As shown in Fig. 5b, the accelerated lifetime show that the obvious increase of stability by introducing $TiO_2$-NTA interlayer. Both the Ti/$TiO_2$-NTA/NATO anode and the Ti/blue-$TiO_2$-NTA/NATO anode achieve 2–3 h of the destructive testing. Compared to the 0.4 h of Ti/NATO anode, the accelerated lifetime of the Ti/blue-$TiO_2$-NTA/NATO anode has increased by 7 times, which indicates a great potential for the industrial application.

Degradation experiments with phenol were used to quickly distinguish the anodic oxidation capacity of the different electrodes. As shown in Figs. 6a and b, the degradation and TOC removal of phenol by Ti/blue-$TiO_2$-NTA/NATO anode is better than Ti/NATO and Ti/$TiO_2$-NTA/NATO anodes, which proves that the anodic oxidation ability was improved by the blue-$TiO_2$-NTA inter layer. To further demonstrate that the increase of $O_3$ promotes the generation of $^{\bullet}OH$, it is necessary to measure the concentration of ROS.

The determination of anodic $O_3$ and cathodic $H_2O_2$ production was investigated in a dual-chamber ORR-EO, according the determination methods described in our former work [10]. As shown in Fig. 7, the concentration of dissolved $O_3$ in Ti/NATO anode chamber was saturated at around 10 mg/L after 120 min of electrolysis, whereas it saves 30 min to reach 10 mg/L of saturated $O_3$ by Ti/blue-$TiO_2$-NTA/NATO anode, which proved the Ti/blue-$TiO_2$-NTA/NATO anode behave a higher $O_3$ generation ability. $H_2O_2$ accumulation could reach over 900 mg/L in the CNTs-C/PTFE cathode chamber after 180 min of electrolysis, which ensured peroxone process could continually occur by consuming dissolved $O_3$. The above results are consistent with the pattern of phenol degradation and TOC removal, and it can be predicted that the $^{\bullet}OH$ would increase in Ti/blue-$TiO_2$-NTA/NATO anode and CNTs-C/PTFE cathode combined ORR-EO system.

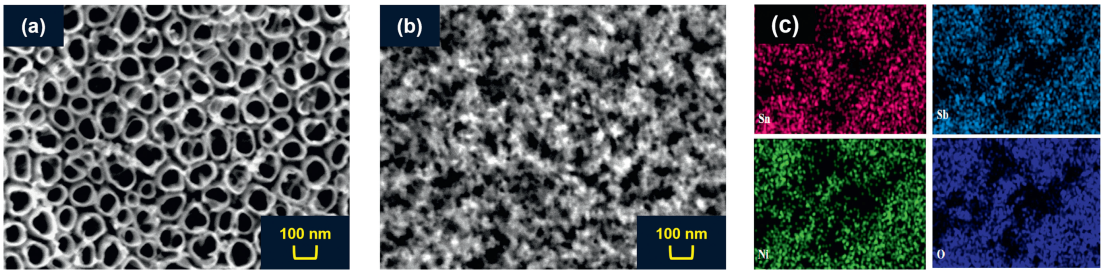

**Fig. 4.** SEM images of the (a) blue-$TiO_2$-NTA inter layer, (b) NATO catalyst layer, and (c) EDS mapping of NATO catalyst layer.

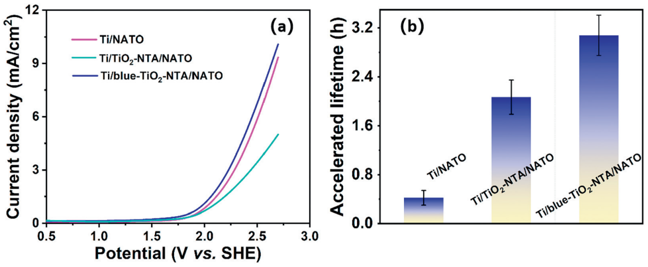

**Fig. 5.** The (a) LSV curves and (b) accelerated lifetime of Ti/NATO, Ti/$TiO_2$-NTA/NATO and Ti/blue-$TiO_2$-NTA/NATO anodes.

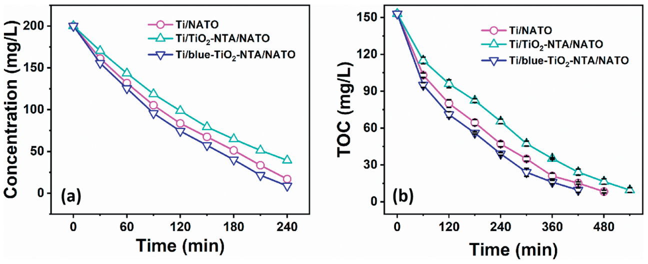

**Fig. 6.** The removal of (a) phenol and (b) TOC by Ti/NATO, Ti/$TiO_2$-NTA/NATO and Ti/blue-$TiO_2$-NTA/NATO anodes combined with CNTs-C/PTFE cathode.

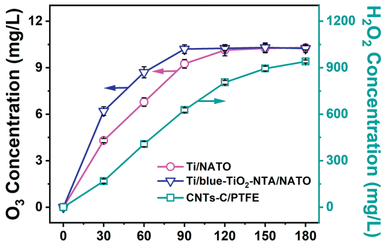

**Fig. 7.** The generation of $O_3$ by Ti/NATO anode, Ti/blue-$TiO_2$-NTA/NATO anode and $H_2O_2$ by CNTs-C/PTFE cathode.

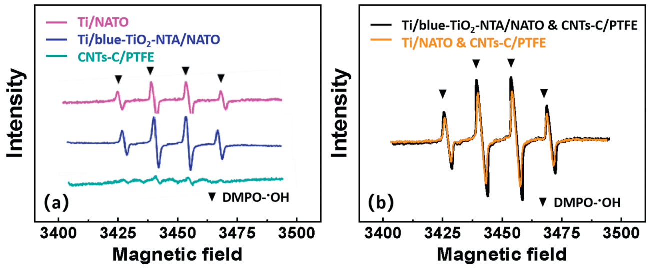

**Fig. 8.** ESR signal of $^{\bullet}$OH in a dual-chamber ORR-EO: (a) Respective and (b) mixed solution from two chambers.

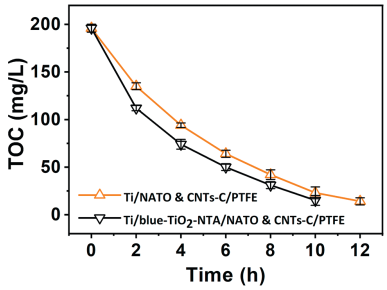

**Fig. 9.** The removal of TOC in landfill leachate bio-effluent by Ti/blue-$TiO_2$-NTA/NATO anode and CNTs-C/PTFE cathode combined ORR-EO.

ESR was adopted to verify and detected *in situ* generations of $^{\bullet}$OH [24] by using a dual-chamber electrolysis cell. Additionally, other species of ROS, such as $^{\bullet}O_2^-$, $^1O_2$, and organic radicals [25,26] were not detected in this system. As shown in Fig. 8a, CNTs-C/PTFE cathode could produce a little of $^{\bullet}$OH. In comparison, the signal of $^{\bullet}$OH by Ti/blue-$TiO_2$-NTA/NATO anode was significant, and it was a little higher than that of Ti/NATO anode. Peroxone synergistic effect in ORR-EO system was proved by determine the mixture of anode and cathode chambers. As shown in Fig. 8b, Ti/blue-$TiO_2$-NTA/NATO anode and CNTs-C/PTFE cathode combined ORR-EO system performed a highest signal of $^{\bullet}$OH. In conclusion, the introduction of blue-$TiO_2$-NTA inter layer enhanced the $^{\bullet}$OH generation through both the $O_3$ evolution and peroxone process.

Results in Fig. 9 demonstrate that Ti/blue-$TiO_2$-NTA/NATO anode and CNTs-C/PTFE cathode combined ORR-EO system removed 92% of TOC in the leachate bio-effluent during a 10-h treatment, while the TOC removal efficiency was improved by 16.7% than Ti/NATO anode and CNTs-C/PTFE cathode combined ORR-EO system. The results prove that the performance improvement of the ORR-EO system after the introduction of the Ti/blue-$TiO_2$-NTA/NATO anode is also applicable to the actual wastewater. Based on Eq. 1, the predicted energy consumption is approximately 45 kWh/$m^3$, indicating significant potential for the deep treatment of industrial wastewater.

In this study, the Ti/blue-$TiO_2$-NTA/NATO as an efficient and long-lasting anode was successfully introduced into the ORR-EO system. When combined with CNTs-C/PTFE air cathode, the synergistic peroxone effect by anodic product $O_3$ and cathodic product $H_2O_2$ accelerated the formation of $^{\bullet}$OH. The anodic oxidation and peroxone process demonstrated a high degradation ability for both phenol and real industrial wastewater at a relatively low energy cost. It has great potential for application in leachate bio-effluent treatment and could replace membrane processes since it eliminates the further treatment for leachate concentrates.

## Declaration of competing interest

The authors declare that they have no known competing financial interests or personal relationships that could have appeared to influence the work reported in this paper.

## Acknowledgment

This work was financially supported by grants from the National Natural Science Foundation of China (No. 52070008).

## References

[1] C. Zhang, H. Chen, G. Xue, et al., J. Clean. Prod. 321 (2021) 128971.
[2] H. Wang, J. Zhan, W. Yao, et al., Water Res. 130 (2018) 127–138.
[3] C. Qu, N. Ren, S. Zhang, et al., Chemosphere 272 (2021) 129453.
[4] G.S. Soomro, C. Qu, N. Ren, et al., Environ. Res. 183 (2020) 109249.
[5] L. Wu, Z. Li, S. Huang, et al., Environ. Int. 127 (2019) 452–461.
[6] H. Olvera-Vargas, N. Gore-Datar, O. Garcia-Rodriguez, S. Mutnuri, O. Lefebvre, Chem. Eng. J. 404 (2021) 126524.
[7] F. Deng, H. Olvera-Vargas, O. Garcia-Rodriguez, et al., J. Hazard. Mater. 377 (2019) 249–258.
[8] C. Qu, D. Liang, J. Environ. Chem. Eng. 10 (2022) 107896.
[9] C. Qu, S. Lu, D. Liang, et al., J. Hazard. Mater. 364 (2019) 468–474.
[10] C. Qu, Y. Li, S. Meng, et al., J. Hazard. Mater. 434 (2022) 128923.
[11] M. Luo, J. Yang, X. Li, et al., Chem. Sci. 14 (2023) 3400–3414.
[12] Z.Y. Zhang, H. Tian, L. Bian, et al., J. Energy Chem. 83 (2023) 90–97.
[13] M. Abbasi, J. Bäckström, A. Cornell, J. Electrochem. Soc. 165 (2018) H568.
[14] Y. Zhang, Y. Yang, S. Yang, E. Quispe-Cardenas, M.R. Hoffmann, ACS ES&T Eng. 1 (2021) 1236–1245.
[15] C. Kim, S. Kim, J. Lee, J. Kim, J. Yoon, ACS Appl. Mater. Interfaces 7 (2015) 7486–7491.
[16] X. Qian, L. Xu, Y. Zhu, H. Yu, J. Niu, Chem. Eng. J. 420 (2021) 127615.
[17] C. Yang, S. Shang, X. Li, Sep. Purif. Technol. 258 (2021) 118035.
[18] C. Meng, Q. Zhuo, A. Wang, et al., Electrochim. Acta 430 (2022) 141055.
[19] K. Wang, K. Zhao, X. Qin, et al., J. Hazard. Mater. 424 (2022) 127747.
[20] Z. Zhao, J. Zhang, J. Yao, S. You, Environ. Res. 210 (2022) 113004.
[21] J. Cai, M. Zhou, Y. Pan, X. Du, X. Lu, Appl. Catal. B 257 (2019) 117902.
[22] L. Xu, J. Niu, H. Xie, et al., J. Hazard. Mater. 402 (2021) 123530.
[23] C. Qu, G.S. Soomro, N. Ren, et al., J. Hazard. Mater. 384 (2020) 121398.
[24] F. Chen, L. Liu, J. Chen, et al., Water Res. 191 (2021) 116799.
[25] F. Chen, L. Liu, J. Wu, et al., Adv. Mater. 34 (2022) 2202891.
[26] J. He, Y. Chen, L. Zhang, et al., Chin. Chem. Lett. 34 (2023) 107344.